Cell-Vertex, Multigrid Euler Scheme for Use with Multiblock Grids

M. T. Arthur* and T. A. Blaylock*
Royal Aerospace Establishment, Farnborough, Hants, England, United Kingdom
and
J. M. Anderson†
University of Glasgow, Glasgow, Scotland, United Kingdom

The feasibility of developing a cell-vertex, finite-volume scheme with multigrid acceleration for use in conjunction with multiblock grids is investigated. The aim is to provide a fast, accurate method for calculating the inviscid flow over complex geometries without the need to modify the computer programs for each new case. For the investigation, a method has been developed for two-dimensional flows, although a grid generator is available for three-dimensional shapes. The method has been validated by comparing results with those from an equivalent, single-block computer program for a case where that is possible. In addition, results are presented from a calculation using a realistic, multiblock grid for a two-element aerofoil configuration. It is concluded that a cell-vertex, multigrid scheme for use with grids having an irregular, multiblock structure can be developed successfully. However, a degree of flexibility in the flow algorithm is needed if the potential benefits of multigrid and multiblock are to be achieved.

Introduction

THE purpose of the work described in this paper is to investigate the feasibility of developing a cell-vertex, finite-volume scheme with multigrid acceleration for use in conjunction with multiblock grids of the form developed by Shaw et al.[1] These methods for grid generation and flow calculation are two of the major developments in computational fluid mechanics in recent years and offer the possibility of providing a fast, accurate method for calculating flows over complex geometries without the need to modify the computer programs for each new case.

In the multiblock grid generation scheme adopted for the present work, the physical space is divided into nonoverlapping regions or blocks each of which can be mapped to a cube in computational space. A block is characteristically associated with a particular component of the configuration such as a wing or flap. In the first stage of the scheme, the way in which the space is divided, that is, the topology of the block structure, is specified. This is a nontrivial task since the specified topology determines the form of grid that will be generated. The objective is to specify a topology that not only will suit the configuration in a general sense, enabling a satisfactory grid to be generated throughout the field, but also will lead to a grid of the desired form around each component of the configuration, for example, an 'O' or 'C' grid around a wing section. The chosen topology may lead to a grid that contains irregular points even though, within each block, the grid is regular (i.e., conventionally structured). In two dimensions, a normal point of the grid is surrounded by four cells, but the irregularity manifests itself by the appearance of points surrounded by three, five, or more cells; the flow algorithm can detect and treat such points appropriately.

Several authors[2,3] have developed grid-generation schemes similar to that just described. Different constraints are sometimes applied at the block boundaries, and details of the methods for generating the grids within blocks may vary, but these schemes yield grids of the same form as those used in the present method.

Alternative methods for generating grids suited to complex configurations have been reported by many authors. Some of these methods yield grids with a blocklike structure, but the blocks may not be rectangular, or the grid within each block may be generated independently of the grids in other blocks, leading to a lack of continuity at block boundaries. For example, Dannenhoffer and Baron[4] use solution-adapted grid embedding to produce desired grid-point densities in regions of high-flow gradients. This procedure makes efficient use of grid points but leads to irregularly shaped blocks, and Dannenhoffer has been forced to use a cell-based data structure such as would be necessary for a completely irregular grid. More recently, Ni and Bogoian[5] have reported a method for calculating multistage turbine flows in which grids in adjacent blocks move relative to each other. Clearly there can be no grid-line continuity at internal block boundaries in such a case, and so a completely different approach to the calculation of the flow at these boundaries must be adopted.

All these schemes differ from some others that have also been called multiblock but that essentially provide a means for dividing the physical space into blocks of a size such that the associated data will fit into the available computer memory. In such schemes, the criteria for dividing the space are completely different from those of the present scheme and the blocks are not necessarily associated with particular components of the configuration; the two types of method are substantially different.

Two significant features of the multiblock scheme referred to here are that 1) the grid lines are continuous across block boundaries and 2) only one type of flow boundary condition may be applied at a given block boundary. The latter condition means that at least three blocks are required for a single aerofoil calculation, and a grid of that form is used for the validation of the method described in this paper. It may be noted that although not required by the flow calculation method, the slopes of the grid lines are normally also continuous across block boundaries unless constraints have been placed on the positions of the boundaries themselves.

The scheme has been developed for the generation of grids in three dimensions, but the results presented in this paper are

Presented as Paper 89-0472 at the AIAA 27th Aerospace Sciences Meeting, Reno, NV, Jan. 9-12, 1989; received June 23, 1989; revision received April 26, 1990; accepted for publication April 28, 1990.

*Research Scientist.

†Summer Intern.

for calculations of two-dimensional flows. The grid used for the two-element aerofoil calculations was obtained from a cut through a three-dimensional grid.

The second of the developments combined in the work presented here is the cell-vertex, multigrid method applied to systems of hyperbolic equations. This technique was pioneered by Ni[6] for solving the Euler equations for steady flow and yielded significant improvements in speed and accuracy over existing methods. The scheme uses Lax-Wendroff time-stepping and, in contrast to cell-centered schemes, is formally second-order accurate except in the neighborhood of shock waves, even for nonsmooth grids. Ni's scheme has a further advantage in that it has fewer possible spurious modes than cell-centered schemes.[7] It should be noted that all schemes of this type (i.e., not upwinded) require the addition of some form of smoothing or artificial dissipation to ensure stability, and this may reduce the accuracy of the scheme. The cell-vertex method has been developed extensively by Hall[8] and Arthur,[9] and it is the latter development that forms the basis of the present work. It is intended that the flow calculation method should be quite general, in the sense that it should enable the flow over any configuration to be calculated, given a grid of the multiblock type, without modification to the computer program. Since multiblock grids may contain blocks with very different numbers of intervals in different coordinate directions and with large variations between blocks, the method has been developed with the following features to enable the benefits of multigrid to be realized:

1) In each block, the ratio of the number of intervals in one grid to that in the grid one level coarser may be any integer rather than the more usual restriction to two; furthermore, the integer may be different in the different coordinate directions and may vary from block to block.

2) The number of multigrid levels may vary from block to block.

These features mean that although the fine grid is continuous throughout the computational domain, the coarse grids need not be continuous across block boundaries. There is no unique way of developing a cell-vertex multigrid scheme within a multiblock framework, but the desirability of the above features led to the particular choice that is described below.

The methods of Amendola et al.[2] and Fritz et al.,[3] which use grid structures similar to those of the present method, are based on cell-centered Jameson-type schemes[10] for solution of the flow equations. The treatment of internal block boundaries in such schemes is very different from that of the present method, and in particular, no special treatment is required at irregular points of the grid in a cell-centered scheme.

In contrast, the schemes of Dannenhoffer and Baron[4] and Ni and Bogoian[5] use the cell-vertex formulation for solution of the flow equations but have grid structures rather different from those of the present scheme, and, as a consequence, different implementations of the cell-vertex scheme at block boundaries. In the work reported here, the solution is updated during the fine-grid time-step at points on block boundaries in an identical way to that used at interior points of the block, just as if the boundary had not been there. The price that has to be paid is in additional programming logic. For the coarse-grid time-steps of a multigrid sequence, different schemes are used at internal and block-boundary points. This allows greater flexibility but does not, of course, affect the final solution, although it may affect the rate of convergence.

The data associated with the present scheme consist essentially of two parts. The first consists of the grid coordinates, the dependent flow variables and variables used at intermediate stages of the calculation. All the data are held in the computer's main memory and are stored block by block, in a regular, block-structured manner. The blocks may be numbered in any order, but information about the block numbers and relative orientations of adjacent blocks is also held in memory; this constitutes the second part of the data.

Two sets of results are presented to demonstrate the feasibility and potential of the method. The basic feasibility is demonstrated through results of calculations over the aerofoil RAE 2822 for Mach number $M = 0.75$ and angle of incidence $\alpha = 3.0$ deg. These are compared directly with those obtained using an equivalent, single-block method, and since this is a standard test case,[11] they may be compared with results from many other sources.

The second set of results is for the calculation of low-speed flow ($M = 0.2$) over the Williams-A aerofoil-plus-flap configuration, which has a 30-deg flap angle.[12] The grid used for these calculations is irregular in the sense described above, so there are no results from single-block methods using the same grid with which the new results can be compared.

Cell-Vertex, Multigrid Scheme for a Regular Grid

Details of the original scheme and some of its developments have been reported extensively elsewhere (see, for example, Refs. 6, 8, and 9), so only a brief review is given here. The essence of the scheme is that the values of the flow variables are held at grid points—the cell vertices—and integrals around cell boundaries are used to calculate changes in conserved quantities. A Lax-Wendroff time-marching scheme is used to advance the solution towards the steady state, and a multiple grid technique used to accelerate the convergence. In the present formulation, each coarse grid of a sequence is obtained from the grid one level finer by retaining every nth point where n is, in principle, any integer; furthermore, n may be different for each coordinate direction and for each of the grids of the sequence. The only restriction is that n must be greater than 1 for all coordinate directions for the first coarse-grid level of a multigrid sequence.

Since only steady-flow solutions are sought, it is sufficient to assume constant stagnation enthalpy and to solve equations for the conservation of mass and momentum only; the pressure may be obtained directly from Bernoulli's equation. For simplicity, the discussion is restricted to two-dimensional flow, but the extension to three dimensions is straightforward. The differential equations may be written conveniently in conservation form for orthogonal, Cartesian coordinates x and y as

$$\frac{\partial U}{\partial t}+\frac{\partial F}{\partial x}+\frac{\partial G}{\partial y}=0 \tag{1}$$

where U, F $(U_1,\ U_2,\ U_3)$ and $G(U_1,U_2,U_3)$ are vectors with components

$$U=\begin{pmatrix}U_1\\U_2\\U_3\end{pmatrix}=\begin{pmatrix}\rho\\\rho u\\\rho v\end{pmatrix},\quad F=\begin{pmatrix}\rho u\\\rho u^2+p\\\rho vu\end{pmatrix},\quad G=\begin{pmatrix}\rho v\\\rho uv\\\rho v^2+p\end{pmatrix}$$

Bernoulli's equation may be written as

$$(\gamma-1)/2\ (u^2+v^2)+(\gamma p/\rho)=\mathrm{const}$$

The freestream at zero angle of incidence is in the direction of x increasing, while y is positive upwards; ρ and p denote the density and pressure; u and v represent Cartesian velocity components in the x and y directions, respectively, and γ is the ratio of specific heats of a perfect gas, taken to be 1.4.

The Lax-Wendroff formulation for advancing the solution on a fine grid is obtained by expanding U in a Taylor series about the current time level t^n and substituting for $\partial U/\partial t$ from Eq. (1):

$$\delta U^{n+1}=-\left(\frac{\partial F}{\partial x}+\frac{\partial G}{\partial y}\right)\delta t^{n+1}$$
$$-\frac{1}{2}\left[\frac{\partial}{\partial x}\left(\frac{\partial F}{\partial U}\frac{\partial U}{\partial t}\right)+\frac{\partial}{\partial y}\left(\frac{\partial G}{\partial U}\frac{\partial U}{\partial t}\right)\right]^n(\delta t^{n+1})^2\ +0[(\delta t^{n+1})^3] \tag{2}$$

Here, $\delta U^{n+1} = U^{n+1} - U^n$ and the local time-step length is $\delta t^{n+1} = t^{n+1} - t^n$, where $U^n = U(t^n)$; $\partial F/\partial U$ is a symbolic representation of the Jacobian $\partial(F_1, F_2, F_3)/\partial(U_1, U_2, U_3)$ and should not be taken to imply that F is a function of U.

The change δU^{n+1} that is to be associated with a particular grid point is given by an average of the values of the terms on the right of Eq. (2). The average is obtained by integrating over a region surrounding the grid point in question, and since each of the terms is in divergence form, the double integrals involved may conveniently be converted to boundary integrals and evaluated from known values of the integrands at points of the boundary.

A different Taylor series is used to develop the scheme for multigrid acceleration. It relates changes in U at consecutive time levels and may be written[9]

$$\delta U^{n+1} = \delta U^n \frac{\delta t^{n+1}}{\delta t^n} - \frac{1}{2}\left[\frac{\partial}{\partial x}\left(\frac{\partial F}{\partial U}\delta U^n\right) + \frac{\partial}{\partial y}\left(\frac{\partial G}{\partial U}\delta U^n\right)\right]$$
$$\times \frac{\delta t^{n+1}}{\delta t^n}(\delta t^{n+1} + \delta t^n) + 0[(\delta t^n)^2\delta t^{n+1},(\delta t^{n+1})^3] \tag{3}$$

In determining the change to be associated with a particular grid point, a simple algebraic average of the first term on the right over a region surrounding the grid point is used; the second-order term is treated in a similar fashion to that used for the fine-grid time-step. One multigrid cycle consists of a single time-step on the fine grid, followed by one time-step on each of the successively coarser grids of the multigrid sequence, the calculated changes being interpolated back to the fine grid. It should be noted that when the solution is converged on the fine grid, no changes will be generated on the coarser grids, and in the absence of artificial dissipation, the solution would be second-order accurate in space.

Boundary conditions are applied in a manner that is consistent with the scheme for an interior grid point. A flow-tangency condition is applied at a solid surface, while in the far field, the condition is obtained from the freestream together with a compressible vortex of strength determined by the aerofoil lift.

To further increase the rate of convergence to the steady state, the method uses local time-step lengths—estimated maximum lengths permitted by stability considerations for each cell.

Finally, a smoothing increment is added to the solution at each point after each fine-grid time-step so that the scheme can be made stable and to damp spatial oscillations that would otherwise occur, especially in the neighborhoods of shock waves. To satisfy the demands made on it, the form of increment that has been chosen provides some background smoothing but strong smoothing in regions around shock waves.

Cell-Vertex, Multigrid Scheme for Multiblock Grids

In the present scheme, in which fine-grid lines are continuous across block boundaries, the grid in the neighborhood of any grid point will not appear different from a single-block grid, except at block corners where the number of blocks meeting differs from four. In the absence of such irregular points, therefore, it would be possible to construct a multigrid, multiblock algorithm that exactly simulated the single-block method. Furthermore, with an appropriate extension for the treatment of irregular points, one might reasonably expect to obtain a method that yielded results of equal accuracy and with equal rate of convergence as the original scheme. However, such a scheme would have several limitations when applied to general multiblock grids since, by definition, it would require the same number of multigrid levels in all blocks. It has been shown[8] that having four, five, or more levels increases the rate of convergence. Ideally, therefore, each block of the grid should have a number of intervals in each coordinate direction that allows cells to be grouped together to form such a sequence of coarser grids. Experience shows that this is not always easy to achieve, although clearly if coarser grids may be formed from finer grids by taking a number of intervals different from two in each coordinate direction, then the task is made much more easy. However, such flexibility may still be insufficient to enable suitable multigrid sequences to be defined since large blocks might support several multigrid levels while a small block (e.g., 4 cells × 6 cells) can support perhaps only one coarse-grid level, and a wide range of block sizes occurs in a typical multiblock grid. In the large blocks, it is not possible to jump from the fine grid to a very coarse grid in one step since this could lead to instability, especially if the coarse-grid cells have a much higher aspect ratio than those of the fine grid. Such considerations lead one to the development of a scheme that permits different numbers of multigrid levels in different blocks of the field. This is incompatible with the ideas of simulating the single-block algorithm and one is forced to consider schemes in which one or more cycles of time-steps are taken at each point of one block before continuing with a second block, and so on. In such a scheme, care will be needed in the treatment adopted for points on interior block boundaries. Furthermore, instabilities must be expected to develop if the differences in the numbers of multigrid levels in adjacent blocks are such as to lead to solutions being advanced by excessively different amounts of time per cycle at adjacent points. The purpose of the work described here is to investigate the possibility of developing a cell-vertex, multigrid, multiblock scheme that will satisfy the demands made on it in the face of these difficulties.

A common feature of all the types of schemes discussed above is that a single fine-grid time-step is taken in each cycle at each grid point. It is possible and, in fact, beneficial for this time-step to be taken at all points of the field before any coarse-grid time-steps are taken since, with the simple extension described below to deal with irregular points of the grid, the equivalent part of the single-block algorithm can be simulated without incurring a storage penalty. This has the advantage that it removes one source of uncertainty in the method since the single-block scheme is well proven. Such a procedure is adopted in the present work. In the second stage of the scheme, all remaining steps of a cycle are completed for each block in turn.

Treatment at an Irregular Point

Figure 1 shows a region of a multiblock grid in which five blocks meet at a point. Points 1, 2, ..., 11 are cell vertices, and A, B, C, D, and E are cell centroids. Following the procedure for a single-block grid[8] discussed above, the first-order change in U from time level n to time level $n+1$, associated with grid point 1, is [see Eq. (2)] an average value of $-(\partial F/\partial x + \partial G/\partial y)^n\, \delta t^{n+1}$. The average is taken over all cells meeting at the point and is given by

$$(D_1U^n)_1 = -(\delta t^{n+1})_1 \iint\limits_{\substack{\text{cell}\\ 23\ldots(2m+1)}} \left(\frac{\partial F}{\partial x} + \frac{\partial G}{\partial y}\right)^n \mathrm{d}x\mathrm{d}y \Big/ \iint\limits_{\substack{\text{cell}\\ 23\ldots(2m+1)}} \mathrm{d}x\mathrm{d}y$$

The number of cells meeting at grid point 1 is m, and the notation assumes that the numbering convention of Fig. 1 is used. The numerator is evaluated by application of Green's theorem in the plane and the trapezoidal rule. The denominator is simply the area of the cell.

The second-order change in the solution at grid point 1 is an average of the second term on the right of Eq. (2). Here, however, the average is taken over the cell formed by the centroids and is

$$(D_2U^n)_1 = -\frac{1}{2}\left(\delta t^{n+1}\right)_1^2 \iint\limits_{\substack{\text{cell}\\ A_1A_2\ldots A_m}} \left[\frac{\partial}{\partial x}\left(\frac{\partial F}{\partial U}\frac{\partial U}{\partial t}\right)\right.$$
$$\left. + \frac{\partial}{\partial y}\left(\frac{\partial G}{\partial U}\frac{\partial U}{\partial t}\right)\right]^n \mathrm{d}x\mathrm{d}y \Big/ \iint\limits_{\substack{\text{cell}\\ A_1A_2\ldots A_m}} \mathrm{d}x\mathrm{d}y$$

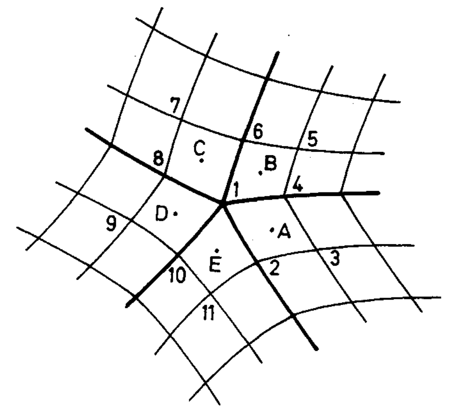

Fig. 1 Region of a fine grid in which five blocks meet at a point.

where in the case illustrated $m = 5$, and A_k represents A, B, C, D, or E as k takes values 1, 2, 3, 4, or 5, respectively. $\partial F/\partial U$ is evaluated directly from approximate values of U at cell centroids given for point A as an example by

$$(U)_A = 0.25(U_1 + U_2 + U_3 + U_4)$$

where $\partial U/\partial t$ is replaced without loss of formal accuracy by $\Delta U^n/\delta t^{n+1}$, where $(\Delta U^n)_{A_k}$ is the contribution to the first-order change $(D_1U^n)_1$ from the cell with centroid A_k and is given for $k = 1$ by

$$(\Delta U^n)_A = -(\delta t^{n+1})_1 \iint_{\substack{\text{cell}\\1234}} \left(\frac{\partial F}{\partial x} + \frac{\partial G}{\partial y}\right)^n \mathrm{d}x\mathrm{d}y \Big/ \iint_{\substack{\text{cell}\\1234}} \mathrm{d}x\mathrm{d}y$$

The expression for $(D_2U^n)_1$ is evaluated in the same manner as that used for the first-order term.

Boundary Conditions

There are effectively five different types of boundary conditions that can be applied at block edges: solid surface, inflow, outflow, and two conditions associated with continuous flow across boundaries in the interior of the field. The first of the last two conditions is essentially the case in which the solution at the boundary point is calculated; the second condition is that applied at the same point in the adjacent block. Clearly the solution need not be recalculated but may simply be copied from the original block for which the calculation was done. The boundary conditions are implemented exactly as in the single-block method in cases for which equivalent conditions exist. At the continuous flow boundaries, the effect of applying the boundary condition is the same as if the point had been an ordinary field point.

The five types of boundary conditions lead to 15 different conditions that can arise at block corners, and they must be dealt with appropriately. The conditions that are dealt with in the existing single-block method and several others that can be treated in a similar way are not described here. Their treatment is a straightforward combination of the two conditions applied along the edges forming the corner. A case that is not in this category is that of a corner formed by two continuous flow boundaries, and this will normally occur in one of two circumstances. The first is a point at the end of a solid boundary, such as at the trailing edge of an aerofoil. In this case, the solid surface condition is applied at the point. The second is where several blocks meet at the point, and for this the required procedure has been described above. (If the point in question is not an irregular point [i.e., if four blocks meet at the point], the procedure as described is equivalent to that applied at an ordinary field point.)

From a practical viewpoint, it should be noted that for a general method, extra bookkeeping is required to allow for the different possible relative orientations of adjacent blocks—eight in three dimensions and at least four in two dimensions. At block corners, where the number of blocks meeting at a point is higher, the amount of additional bookkeeping rises accordingly.

Multigrid with Multiblock

The method for updating the solution on the coarse grids—the multigrid acceleration scheme—is the same as in the single-block method[9] for points in the interior of a block or on a solid surface or far-field boundary. A description of the procedure adopted for the remaining points along the edges and in the corners of blocks follows.

Figure 2 shows a region of the interface between two blocks. The primary block is that in which the solution is being updated, and it is assumed here that points of this block are updated before those of the adjacent block in each cycle. Points of the current grid are marked by crosses; the solid lines in the primary block show the grid one level finer, while in the adjacent block, they show one of the coarse grids in that block's multigrid sequence. The dashed lines show the finest grids of current multigrid sequences of the two blocks, continuous across the boundary. The solution at point 1 of the primary block is updated using information from points 1 to 9. Points 5, 6, and 7 need not be points on any of the coarse grids of the adjacent block's multigrid sequence, but they are on the same fine-grid line. Each is chosen in a similar manner that for point 6 is as follows: point 6 lies on the continuation of the fine-grid line through points 2 and 1 and is an equal number of fine-grid intervals from point 1 as is point 2. If this procedure were to place point 6 outside the adjacent block (i.e., beyond the "far" boundary)—which might easily happen when updating the solution at point 1 on a very coarse grid of the primary block—then point 6 is taken to be on the boundary of the adjacent block opposite point 1.

The change in solution at point 1 for the coarse-grid time-step from time level n to time level $n + 1$ is obtained as follows. Let the subscripts A, B, C, and D denote cells 1456, 8167, 9218, and 2341, respectively. Then the first-order contribution to the change may be obtained from Eq. (3) as

$$(D_1U^n)_1 = \frac{\sum\limits_{k=A,\,B,\,C,\,D} (\delta U^n)_k S_k}{\sum\limits_{k=A,\,B,\,C,\,D} S_k} \left(\frac{\delta t^{n+1}}{\delta t^n}\right)_1$$

where $(\ )_1$ denotes a value for grid point 1, S_k is the area of cell k, and $(\delta U^n)_k$ is a simple algebraic average that for cell D is

$$(\delta U^n)_D = 0.25[(\delta U^n)_1 + (\delta U^n)_2 + (\delta U^n)_3 + (\delta U^n)_4]$$

Except for the first coarse grid of a sequence, the values of (δU^n) at points 5, 6, and 7 will not have been calculated. Indeed, since those points may not lie on any of the coarse grids of the adjacent block multigrid sequence, the required

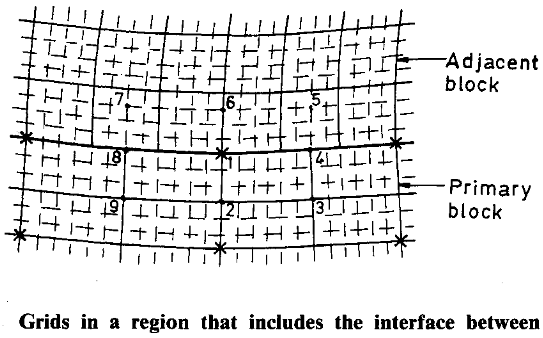

Fig. 2 Grids in a region that includes the interface between two blocks.

increments might not be calculated even as the solution is updated at points of that block. Furthermore, the time-step lengths that are used as the solution is updated in the adjacent block will be those appropriate to the multigrid sequences of that block and may be significantly different from those of the current block. An alternative procedure for obtaining the required values of (δU^n) must be adopted. A simple approximation, suggested by Eq. (3), is given by

$$(\delta U^n)_5 = (\delta U^M)_5 \, \delta t^n / \delta t^M$$

where $(\delta U^M)_5$ is the total change in U at grid point 5 calculated at the most recent fine-grid time-step, and δt^M is the associated time-step length. The superscript n relates to time levels only in the primary block, so δt^n here is an equivalent time-step length based on the primary block grid sequence but relating to grid point 5. Following Ref. 9, time-step lengths used for coarse-grid calculations are related directly to the most recent fine-grid time-step lengths and the relative sizes of coarse and fine grid cells. This differs from the fine-grid procedure in which time-step lengths are calculated from local Courant-Friedrichs-Lewy (CFL) conditions. Thus an approximation to (δU^n) at points 5, 6, and 7 is readily found, and $(D_1 U^n)_1$ may be calculated.

The second-order change $(D_2 U^n)_1$ is an average for cell 3579 of the second term on the right of Eq. (3). Evaluation of the average requires values of $\partial F / \partial U$ and $\partial G / \partial U$ at time level n. They may be obtained directly from known values of U at points 3 and 9, while for points 5 and 7, estimates can be found from approximate values of U obtained by incrementing the values of U calculated at those points during the most recent fine-grid time-step by the values of (δU^n) obtained as described above.

It remains only to consider the method to be applied at points where several blocks meet. Just as the method to be applied on a fine grid was extended for the treatment of irregular points, so the scheme used to update the solution on a coarse grid at a continuous flow boundary, described in the preceding paragraphs, is extended in an analogous way. It is complicated by the different relative orientations and multigrid sequences of the relevant blocks, but the principles of the procedure are a straightforward extension of the schemes already described.

Results

Two sets of results are presented here. The first is to provide validation of the method and to enable an assessment to be made of the features that were included because they were thought necessary if the benefits of multigrid and multiblock were to be exploited. The second set of results is for the calculation of low speed flow over an aerofoil-plus-flap configuration. The results, which were obtained using a multiblock grid containing several irregular points, demonstrate the potential of the method for calculating flows over complex geometries.

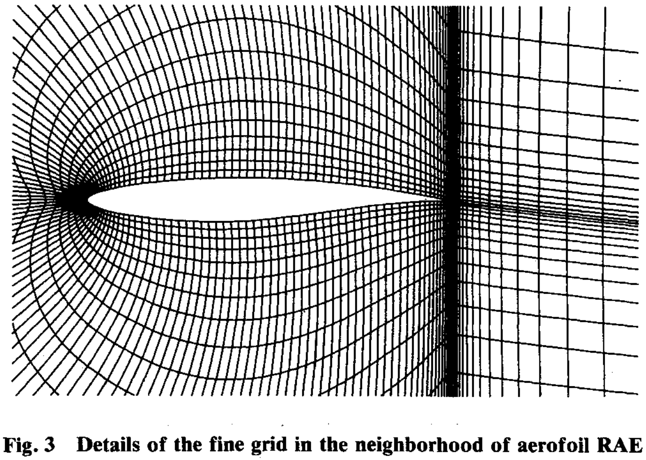

Fig. 3 Details of the fine grid in the neighborhood of aerofoil RAE 2822.

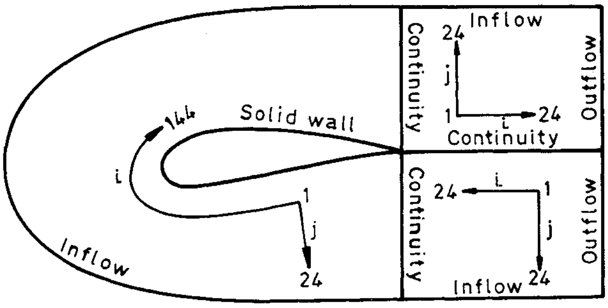

Fig. 4 Block structure for the multiblock aerofoil calculations, showing the numbers of intervals in each coordinate direction and the boundary condition types.

Validation

To validate and assess the performance of the method, it is necessary to choose cases for which the flow can be calculated equally well using an equivalent, single-block method. This eliminates differences that might arise from different Euler algorithms and, in particular, different smoothing schemes. It will also enable the cost of overheads associated with the multiblock grid structure to be assessed directly. For this reason, all calculations in the first set are for the flow over aerofoil RAE 2822 at Mach number $M = 0.75$ and angle of incidence $\alpha = 3$ deg. The flow includes a large supersonic region terminated by a strong shock wave, with the Mach number just upstream of the shock wave exceeding 1.5. The case has been selected as an AGARD test case,[11] so there is an abundance of data with which the present results can be compared.

The high degree of flexibility of the present scheme makes it difficult to demonstrate all the features in a few results. It is hoped that the results provided will allow an overall assessment to be made of the success of the chosen multigrid, multiblock strategy. The information may assist other research workers in developing their own strategies for similar schemes.

The fine grid used in the calculations is a C-grid developed by Hall[13] from a method due to Rizzi.[14] It has 192 intervals in the direction around the aerofoil and 24 into the field; 24 of the 192 intervals are downstream of the trailing edge for both upper and lower parts of the C, leaving 144 on the aerofoil contour. Figure 3 shows the grid in the vicinity of the aerofoil. The outer boundary is approximately eight chords from the aerofoil in all directions. The grid was divided into three blocks for the multiblock calculations and the details of the blocks are shown in Fig. 4.

For reference purposes, one calculation has been done using a single-block method that is, in all other respects, equivalent to the multiblock method described in this report. The calculation was done using the common multigrid sequence in which each coarse grid was obtained from the grid one level finer by omitting alternate points in each coordinate direction. Thus the numbers of intervals in the four grids were 192×24, 96×12, 48×6, and 24×3. It has been found to be advantageous[13] to begin a calculation with some cycles on one or more sequences of grids that omit the finer levels. In this example, 400 cycles were completed using only the two coarsest grids, followed by 300 cycles using a three-level sequence and finally further cycles using all four grids. An equivalent calculation using the three-block grid has also been performed so that housekeeping overheads and other effects on the performance associated with the multiblock method can be determined. Details of the multiblock grid sequences are given explicitly in Table 1, case 1.

The calculated distribution of surface pressure coefficients is shown in Fig. 5, and within plotting accuracy it is the same from both calculations.

The convergence histories of the two calculations are shown in Fig. 6. Two measures of convergence are plotted: the calculated lift coefficient C_L and a measure of the residual, log R_a, where R_a is defined as the mean value of $|\delta\rho/\delta t|$ for all points of the current fine grid; $\delta\rho$ is the change in density at the last fine-grid time-step and δt is the corresponding time-step length. There is clearly no degradation in the performance of the multigrid algorithm in the multiblock method, even though the scheme for updating the solution on the coarse grids at points on block boundaries is formally less accurate than at other points. The spikes in the residual history occur at the changes from the two- to three-level sequence and the three- to four-level sequence. The horizontal dashed line indicates the lift coefficient obtained from the single-block method after an effectively infinite number of cycles. There is a perceptible difference in the converged lift coefficients from the two methods—approximately 0.2%—but for all practical purposes, the converged results are the same.

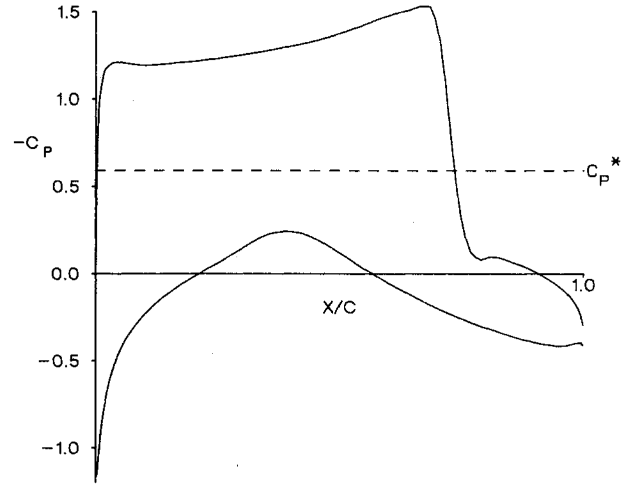

Fig. 5 Calculated surface pressure coefficient distribution for aerofoil RAE 2822, $M=0.75$, $\alpha=3.0$ deg.

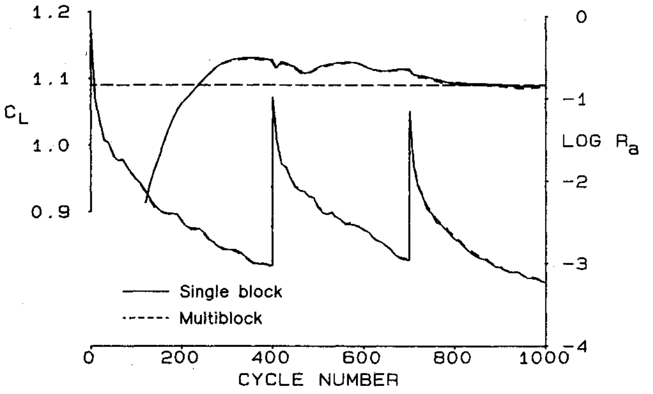

Fig. 6 Convergence histories of the residual and lift coefficient, case 1.

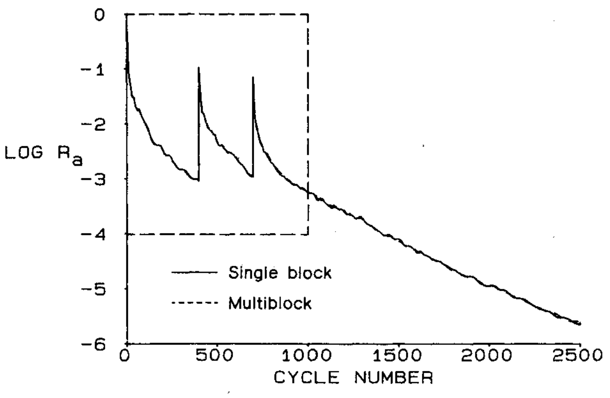

Fig. 7 Convergence history of the residual, case 1.

In Fig. 7, the variation of residual with cycle number is plotted for 2500 cycles, showing that the multiblock method continues to perform well as the calculation converges. It should be noted that far fewer cycles would be required to achieve a level of convergence adequate for practical purposes. The boxed region indicates the portion of the figure shown on a larger scale in Fig. 6.

Figure 8 shows the same information as Fig. 6, but in the former, the convergence histories are plotted against CPU time on a Cray 1S computer. As expected, the CPU time per cycle is greater for the multiblock method. The latter requires 18.1 s to reach a level of convergence at which the lift coefficient does not subsequently deviate by more than 0.5% from the fully converged value—3.3 s or 22% more than is required by the single-block method. This gives an indication of the penalty to be paid for the overhead associated with multiblock grids, although this will, of course vary with the number and sizes of blocks.

Figure 9 shows two further results that may be compared with the one shown in Fig. 8. The solid lines show convergence histories obtained from the multiblock method using the

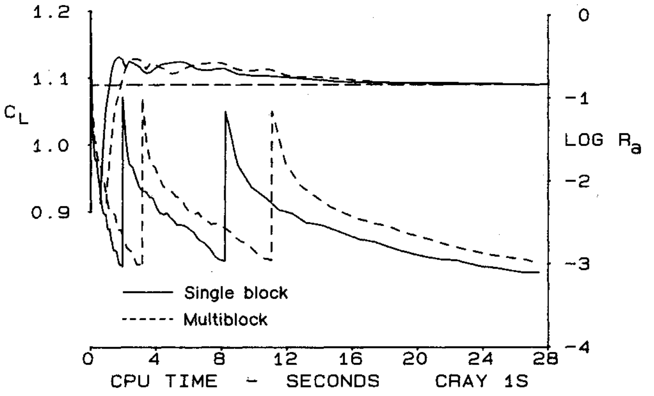

Fig. 8 Convergence histories of the residual and lift coefficient, case 1.

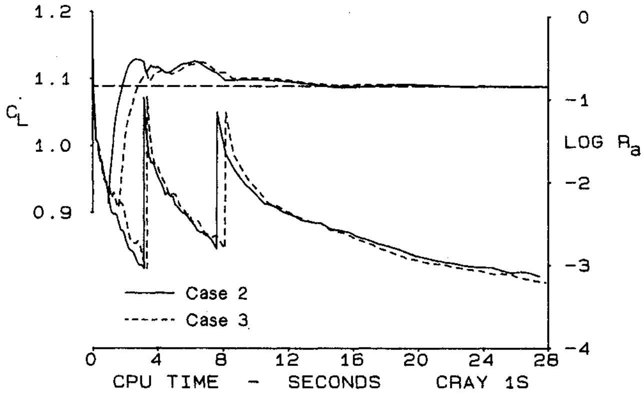

Fig. 9 Convergence histories of the residual and lift coefficient showing the effect of discontinuities in coarse grid lines at block boundaries.

Table 1 Numbers of intervals in each coordinate direction for each grid of each sequence for the various cases investigated

Sequence	Case 1	Case 2	Case 3
		Block 1	
1	6×6 3×3	6×6 3×3	6×6
2	12×12 6×6 3×3	12×12 3×3	12×12 6×6
3	24×24 12×12 6×6 3×3	24×24 6×6 3×3	24×24 6×6
		Block 2	
1	36×6 18×3	36×6 18×3	36×6
2	72×12 36×6 18×3	72×12 18×3	72×12 18×3
3	144×24 72×12 36×6 18×3	144×24 36×6 18×3	144×24 36×6 18×3
		Block 3	
1	6×6 3×3	6×6 3×3	6×6
2	12×12 6×6 3×3	12×12 3×3	12×12 6×6
3	24×24 12×12 6×6 3×3	24×24 6×6 3×3	24×24 6×6

multigrid sequences of case 2. The two-level sequence used for the initial cycles is the same as for case 1, but the first coarse-grid level of the three- and four-level sequences of case 1 has been omitted to produce the grid sequences for case 2. Thus the finest and coarsest grids in each sequence are the same in both cases, but there are four fine-grid intervals per interval of the grid one level coarser in each coordinate direction for the second and third sequences of case 2. The dashed lines show convergence histories for a third set of grid sequences, case 3. The essential feature of these grid sequences is that the coarsest grid used in block 2 is coarser than that of blocks 1 and 3, i.e., the coarse-grid lines are not continuous across block boundaries. To achieve this, the initial time-steps are taken on a single grid. Details of the grid sequences are shown in Table 1.

Comparison of the results from cases 1, 2, and 3 suggests that the multiblock scheme works well with nonstandard grid sequences, different grid sequences in adjacent blocks, different numbers of levels in adjacent blocks, and discontinuities across block boundaries in grid lines of any but the finest grid of a sequence.

In addition to the capabilities already described, the scheme permits the use of multigrid in some blocks with no multigrid in others. Results show that such a strategy will be successful in some cases but will work less well or may even fail if multigrid acceleration is used in most blocks but not some, perhaps close to a solid surface, where the solution changes rapidly during the transient phase. A way of overcoming this breakdown might be, in those blocks where no multigrid is possible, to take several fine-grid time-steps per cycle of time-steps in the remaining blocks. Such a procedure is not possible within the present strategy.

Williams-A Aerofoil Plus Flap

The Williams aerofoil-plus-flap configurations[12] provide testing cases for both the grid-generation and flow-calculation methods, even for the low speed flow, $M = 0.2$, considered here. There are two configurations, A and B, having 30- and 10-deg flap angles, respectively. The former has been selected for the present work. The 30-deg flap angle leads to high suction peaks near the leading edges of both flap and main element. Figure 10 shows the grid in the neighborhood of the configuration, while Fig. 11 gives further details of the region between the two elements. The grid consists of 53 blocks with a total of 6518 cells and four irregular points. There is a C-grid structure around the main aerofoil and a second around the flap; these are embedded in an H grid extending to the farfield, where the outer boundary is rectangular. Some of the (internal) block boundaries are not needed to produce this topological structure, but they have been introduced to provide grid control. The block sizes vary from 26 cells × 15 cells to 5 cells × 5 cells so that, with this grid, little benefit can be obtained from the use of multigrid.

Calculated distributions of surface pressure coefficients are shown in Figs. 12a and 12b. There are few results available with which the present ones can be compared and no general consensus as to their accuracy.[15] The effects of compressibility on the flow over this configuration are significant even at this low Mach number (the peak Mach number approaches 0.8), so a solution obtained using a panel method could not be regarded as definitive. However, the exact incompressible flow solution is known and is shown as the dashed lines in the figures. The peak suction levels appear to be well predicted, although the general suction levels over the upper surface of the flap and towards the trailing edge of the main element are probably a little low.

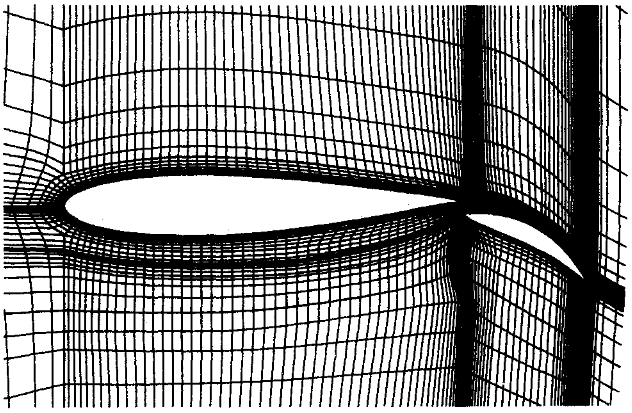

Fig. 10 Details of the grid in the neighborhood of the Williams-A aerofoil-plus-flap configuration.

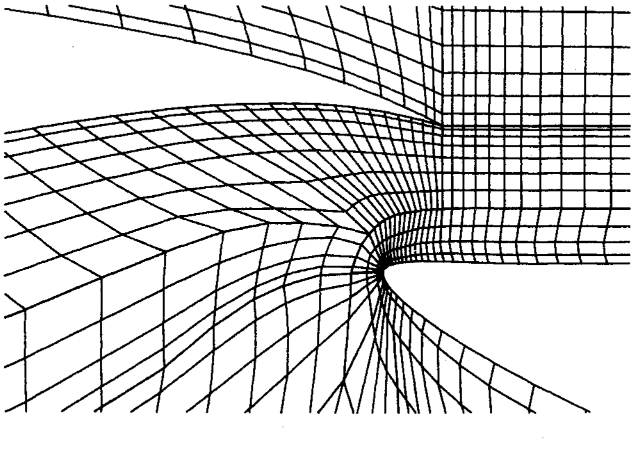

Fig. 11 Details of the grid in the region between the main element and flap of the Williams-A aerofoil.

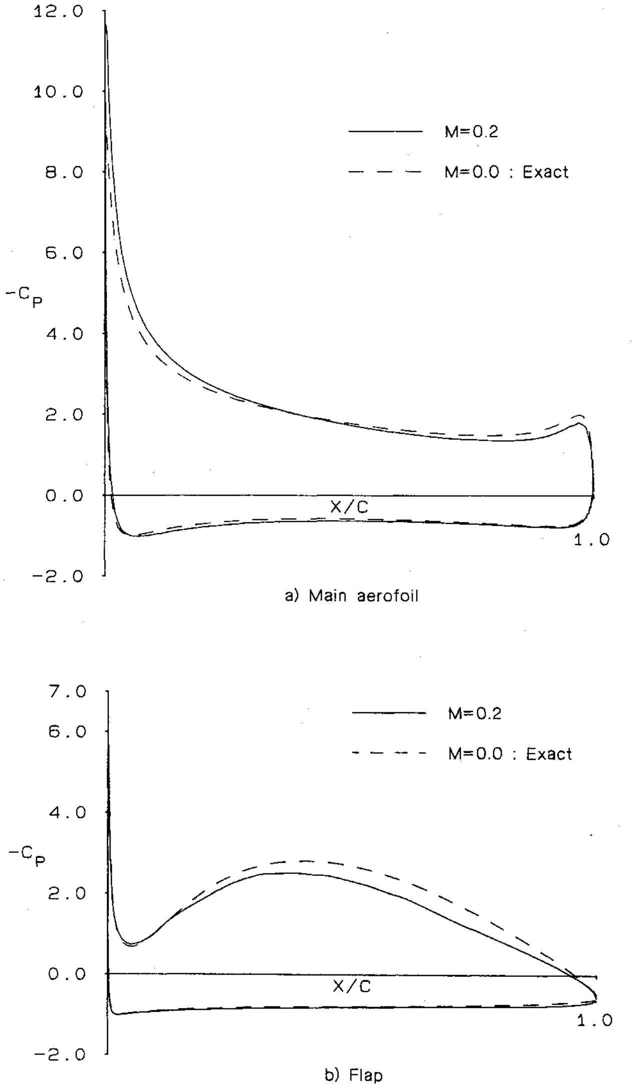

Fig. 12 Calculated distribution of surface pressure coefficients for the Williams-A two-element aerofoil.

A more detailed investigation of the calculated flow in the field shows no problems associated with block boundaries or irregular points of the grid. In some blocks adjacent to solid surfaces, the block size prevented the use of multigrid. The calculation diverged if multigrid was used in other blocks close or adjacent to solid surfaces, so only fine-grid time-stepping was used in all these blocks. Elsewhere in the field, the use of one or more levels of multigrid where possible produced no significant improvement in the convergence rate. Removal of some of those internal block boundaries that were originally introduced purely for grid control purposes, but which are not, in principle, needed for the flow calculation, might lead to faster convergence rates. This has not yet been investigated because of the memory limitations of the Cray 1S. Nevertheless, the results demonstrate that the method can be used to calculate two-dimensional flows over complex shapes, given a grid of the multiblock type. Improvements to the method may lead to greater speed and more accurate predictions of flows such as that presented above for the Williams-A configuration, although it has not yet been possible to determine how much, if any, of any shortcoming is due to deficiencies in the grid. Preliminary investigations show that there is some sensitivity to grid point density and distribution, especially in the overlap region between the two elements.

Conclusions

A strategy has been devised for successfully combining the cell vertex, multigrid and multiblock methods enabling solutions of the Euler equations for flows over complex geometries to be obtained rapidly and accurately. The versatility of the scheme has been demonstrated and validated through calculations of a flow over the aerofoil RAE 2822. The penalty associated with the ability to carry out calculations using grids with multiblock structure is far from negligible. However, since the method enables flows over general two-dimensional shapes to be calculated without changes to the associated computer program, as demonstrated by the results for the Williams-A aerofoil-plus-flap configuration, it is felt that the penalty should prove acceptable.

The success of the present work provides encouragement for the extension of the flow calculation method to three-dimensional flows. In view of the nature of general multiblock grids, it seems essential that the method should allow different numbers of multigrid levels in different blocks. This is probably more important than having flexibility in the way in which coarse grids are obtained from finer grids. However, it is felt that there will be some benefit in modifying the overall strategy so that several fine-grid time-steps can be taken consecutively in one block before further time-steps are taken in another block.

References

[1] Shaw, J., Forsey, C. R., Weatherill, N. P., and Rose, K. E., "A Block Structured Mesh Generation Technique for Aerodynamic Geometries," *Numerical Grid Generation in Computational Fluid Dynamics,* edited by J. Hauser and C. Taylor, Proceedings of the International Conference, Pineridge, Swansea, England, July 14-17, 1986, pp. 329-340.

[2] Amendola, A., Tognaccini, R., Boerstoel, J. W., and Kassies, A., "Validation of a Multi-Block Euler Flow Solver with Propeller-Slipstream Flows," *Validation of Computational Fluid Dynamics,* AGARD CP 437, Vol. 2, Poster Papers, Dec. 1988, Paper 1.

[3] Fritz, W., Haase, W., and Seibert, W., "Mesh Generation for Industrial Application of Euler and Navier-Stokes Solvers," *Three-Dimensional Grid Generation for Complex Configurations - Recent Progress*, AGARDograph AG-309, March 1988, pp. 106-123.

[4] Dannenhoffer, J. F., III, and Baron, J. R., "Robust Grid Adaptation for Complex Transonic Flows," AIAA Paper 86-0495, Jan. 1986.

[5] Ni, R.-H., and Bogoian, J., "Prediction of 3-D Multi-Stage Turbine Flow Field Using a Multiple-Grid Euler Solver," AIAA Paper 89-0203, Jan. 1989.

[6] Ni, R.-H., "A Multiple Grid Scheme for Solving the Euler Equations," *AIAA Journal,* Vol. 20, No. 11, 1982, pp. 1565-1571.

[7] Morton, K. W., and Paisley, M. F., "A Finite Volume Scheme with Shock Fitting for the Steady Euler Equations," *Journal of Computational Physics,* Vol. 80, No. 1, 1989, pp. 168-203.

[8] Hall, M. G., "Cell-Vertex Multigrid Schemes for Solution of the Euler Equations," *Numerical Methods for Fluid Dynamics, II,* edited by K. W. Morton and M. J. Baines, Oxford Univ., London, England, 1986, pp. 303-345.

[9] Arthur, M. T., "A Generalization of Hall's Scheme for Solving the Euler Equations for Two-Dimensional Flows," *Multigrid Methods: Special Topics and Applications,* edited by U. Trottenberg and W. Hackbusch, GMD-Studien Nr. 110, May 1986, pp. 7-23.

[10] Jameson, A., Schmidt, W., and Turkel, E., "Numerical Solution of the Euler Equations by Finite Volume Methods using Runge-Kutta Time Stepping," AIAA Paper 81-1259, June 1981.

[11] Fluid Dynamics Panel Working Group 07, "Test Cases for Inviscid Flow Field Methods," AGARD Advisory Rept. No. 211, 1985.

[12] Williams, B. R., "An Exact Test Case for the Plane Potential Flow about Two Adjacent Lifting Aerofoils," ARC R&M 3717, 1973.

[13] Hall, M. G., "Cell-Vertex Multigrid Solution of the Euler Equations for Transonic Flow Past Aerofoils," Unpublished MOD (PE) report.

[14] Rizzi, A., "Computational Mesh for Transonic Aerofoils," *Numerical Methods for the Computation of Inviscid Transonic Flows with Shock Waves,* edited by A. Rizzi and H. Viviand, Vieweg, 1981, pp. 222-254.

[15] Williams, B. R., private communication, 1988.